THE ASTROPHYSICAL JOURNAL, 469:L101–L104, 1996 October 1

MOLECULAR SPIRAL ARMS IN M31

L. LOINARD,[1,2] T. M. DAME, AND E. KOPER
Center for Astrophysics, 60 Garden Street, Cambridge, MA 02138
J. LEQUEUX
DEMIRM, Observatoire de Paris, 61 Avenue de l'Observatoire, F-75014 Paris, France
P. THADDEUS
Center for Astrophysics, 60 Garden Street, Cambridge, MA 02138
AND
J. S. YOUNG
Department of Physics and Astronomy and Five College Radio Observatory, University of Massachusetts, Amherst, MA 01003
Received 1996 April 3; accepted 1996 July 17

ABSTRACT

We describe a high-resolution, high-sensitivity CO(1–0) survey of a large fraction of the south-west star-forming "ring" 20 kpc in diameter in M31 made with the 14 m FCRAO telescope and its QUARRY receiver array. At the 45″ angular resolution of the telescope, the ring is resolved into giant complexes of molecular gas with typical sizes of a few hundred parsecs and masses in excess to $10^6\ M_\odot$. Most of these delineate a prominent spiral arm coincident with that traced by atomic hydrogen and dust. This arm appears in all respects quite similar to a prominent spiral arm in our Galaxy at about the same Galactic radius: the Carina arm. Closer to the center, a second fainter molecular spiral arm segment with an H I and dust counterpart is also detected. The main OB associations and the UV light define an arm offset from that traced by the gas by about 500 pc. The H II regions are mainly found either along the edge of the prominent gaseous arm which faces the associations, or aligned with the second fainter gaseous arm. They define Baade's arms S4 and S3, respectively.

Subject headings: galaxies: ISM — galaxies: individual (M31) — galaxies: structure — ISM: molecules

1. INTRODUCTION

The relation of molecular gas to spiral structure and other tracers of star-formation is difficult to establish in our own galaxy because of our perspective in the Galactic disk, and so observations of nearby spirals are crucial for examining this issue. As our nearest spiral neighbor, M31 should be the best candidate for such a study; but progress has been slow owing to both its large angular size and its faintness in CO, the best tracer of molecular gas. Although complete surveys of H I (Brinks & Shane 1984) and the IR dust emission (Xu & Helou 1995) have now achieved an angular resolution of 1′ or better, the only existing complete CO survey of M31 has been done with the 1.2 m telescope at the Center for Astrophysics (CfA) at an angular resolution of 8.′7 (Dame et al. 1993). This survey has shown that the total CO luminosity of M31 is weaker than that of the Milky Way by a factor of roughly 6; but owing to the relatively low linear resolution of the CfA survey (1.7 kpc along the major axis), only the large-scale distribution of molecular gas could be determined. Intermediate resolution (100″) observations made with the AT&T 7 m telescope (e.g., Stark, Linke, & Frerking 1981) have shown that the CO emission was largely confined into arm segments 1–2 kpc wide; and higher angular resolution observations of several small selected areas (see references in Kutner, Verter, & Rickard 1990) showed that individual clouds or cloud complexes in M31 could be as strong in CO as those in the Galaxy. These high-resolution studies, however, have all been too limited in coverage or sensitivity to investigate the distribution of molecular clouds and its relation to other tracers of spiral structure along a major portion of a spiral arm.

We have mapped the CO(1–0) emission in a fairly large fraction of the south-west "ring" of M31 at high angular resolution and high sensitivity. This region contains many H II regions (Pellet et al. 1978) and OB associations (Magnier et al. 1993), including the largest OB association in the galaxy: NGC 206. The angular resolution obtained and the large area mapped enable us to perform a study of the relationship between molecular clouds, spiral structure and other tracers of recent star-forming activity.

2. OBSERVATIONS

The observations were obtained from 1995 March to 1996 January using the 14 m radome-enclosed millimeter telescope of the Five College Radio Astronomy Observatory in Amherst (Massachusetts). At the frequency of the $J = 1 \rightarrow 0$ transition of CO, the half-power beamwidth of the telescope is about 45″. This instrument is now equipped with the QUARRY array of 15 Shottky receivers, with which a 30 pixel $5' \times 4'$ map sampled every 50″ (a *footprint*) can be obtained in two pointings. Twenty-one such footprints were observed, corresponding to 630 individual pixels, and to an area of more than 400 arcmin^2 sampled every beamwidth. This sampling provides roughly four times the spatial coverage of Nyquist sampling while degrading the angular resolution only sightly. Numerical experiments with Galactic CO data smoothed to the linear resolution of the 14 m telescope at M31 confirmed that the

[1] Current address: Space Telescope Science Institute, 3700 San Martin Drive, Baltimore, MD 21218.
[2] Observatoire de Grenoble, Laboratoire d'Astrophysique, Université Joseph Fourier, B.P. 53X, F-38041 Grenoble Cedex, France.

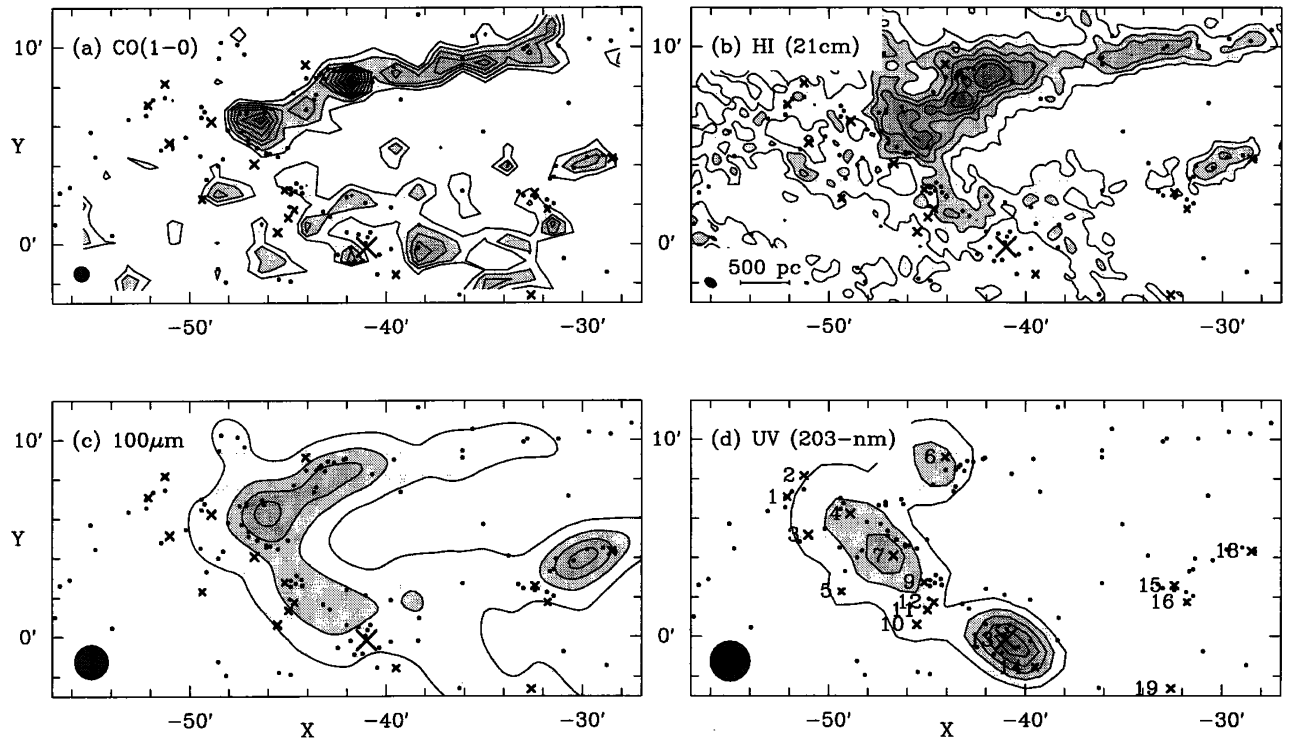

FIG. 1.—(*a*) W_{CO}; the first contour is at 2 K km s^{-1} and the contour interval is 1 K km s^{-1} (T_{mb}). The angular resolution is 45″. (*b*) $W_{H\,I}$ from Brinks & Shane (1984); the first contour is at 250 K km s^{-1} and the contour interval is 100 K km s^{-1} (T_b). The angular resolution is 24″ × 36″ ($\Delta\alpha \times \Delta\delta$). (*c*) *IRAS* 100 μm flux from Xu & Helou (1995); the first contour and the contour interval are 1 MJy sr^{-1}. The angular resolution is 1.′7. (*d*) 203 nm UV image from Milliard (1984); the first contour is at 3×10^{-9} W m^{-2} nm^{-1} sr^{-1} and the contour interval is 2×10^{-9} W m^{-2} nm^{-1} sr^{-1}. The angular resolution is 2′. On the four maps are indicated the OB associations (*crosses*) and the H II regions (*dots*) present in the field. They have been extracted from the catalogs by Magnier et al. (1993) and Pellet et al. (1978), respectively. On Fig. 1*d*, the OB associations are labeled following Magnier et al.

undersampling had a negligible affect on our maps and our conclusions.

The pointing and the focus were checked on standard sources at least twice during each 12 hr observing session; the pointing was found to be accurate to ±7″ rms. The observations were calibrated by means of a standard blackbody chopper wheel. The intensity scale used in this paper is "main beam brightness temperature": $T_{mb} = T_A^*/\eta_{mb}$; the present main beam efficiency η_{mb} of the 14 m telescope is 0.55 at 115 GHz. The spectrometer was a 256 channel autocorrelator providing 80 MHz of available bandwidth at a resolution of 312.5 kHz; at 115 GHz, this yields a velocity resolution of 0.8 km s^{-1} and a total bandwidth of 210 km s^{-1}. Since typical CO lines were 10–30 km s^{-1} wide, the data were Hanning-smoothed to 3.25 km s^{-1} to improve the signal-to-noise ratio. The spectra were obtained by switching between the source and an OFF position taken well outside the molecular disk of M31 but at the same elevation to ensure flat spectral baselines. Including the atmospheric contribution, the system temperatures during the survey varied between 700 and 1500 K; about 100 minutes of integration time were required to achieve an rms noise level of ~22 mK (T_A^*) per 3.25 km s^{-1} channel.

3. DISCUSSION

At the 150 pc linear resolution of the 14 m telescope at 115 GHz, the south-west part of the star-forming ring in M31 is resolved into large complexes of molecular gas (Fig. 1*a*). Most of these are aligned along the prominent spiral arm S4 (Baade 1958), also apparent on the H I and 100 μm infrared maps shown on Figures 1*b* and 1*c*, respectively. No significant offset between the CO and the H I emission is observed (see Figs. 1 and 2). Some CO emission associated with the inner arm S3 can be discerned near $X = -30'$, $Y = +4'$; an arm also seen in H I and far-infrared emission. The shape of the main molecular arm S4 follows very closely that of the dust

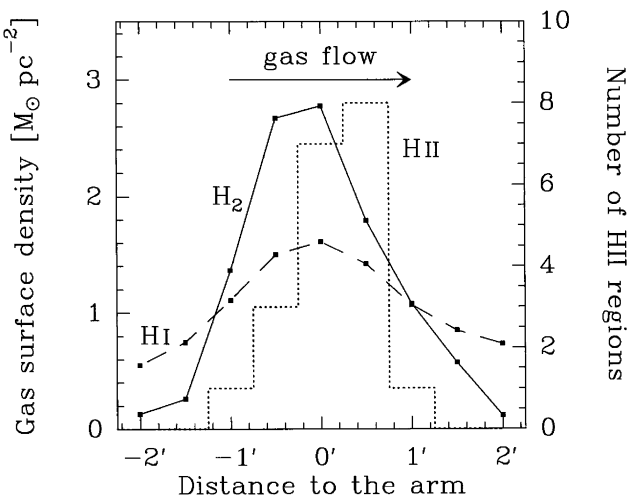

FIG. 2.—Distribution of H_2, H I, and H II regions across the upper part of the arm S4. Nine bins 0.′5 wide running along and parallel to the upper part of the spiral arm S4 were defined. In each bin, the number of H II regions were counted, and the CO and H I integrated intensity were averaged. H_2 and H I column densities were computed as described in the text.

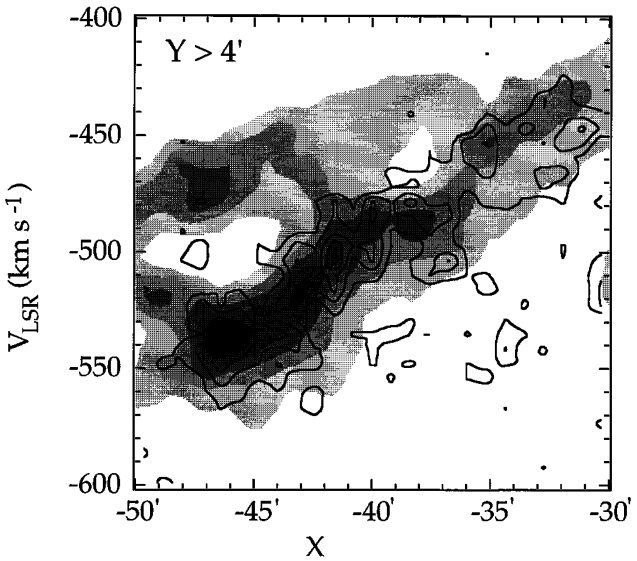

FIG. 3.—Position-velocity maps of CO (*contours*) and H I (*gray scale*) in the upper part of the spiral arm S4 ($Y \leq 4'$). The CO contour interval is 0.015 K, and the spacing between gray levels for the H I is 9.45 K.

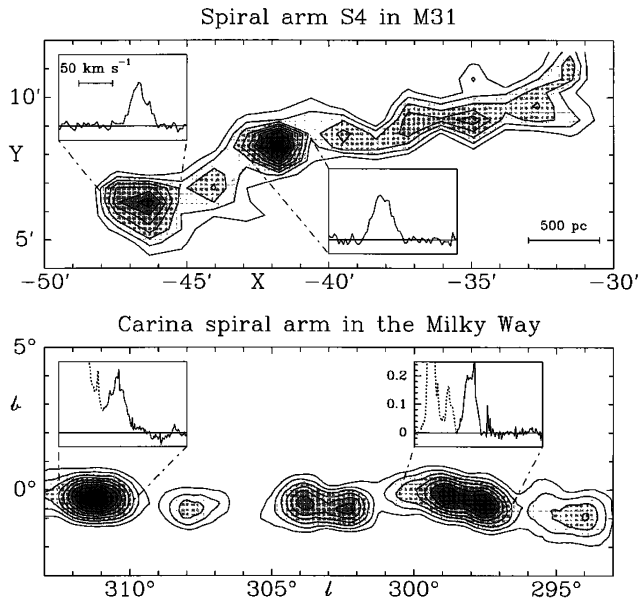

FIG. 4.—Comparison between the molecular spiral arms S4 in M31 and Carina in the Milky Way. The Carina data are from the 1.2 m survey of Grabelsky et al. (1988) and have been smoothed to match our linear resolution in M31 and scaled to T_{mb}. The first contour (2 K km s^{-1}) and the contour levels (1 K km s^{-1}) are the same for both maps. The spectra averaged over four well defined condensations are shown all on the same scales, both in velocity and temperature. The Carina spectra have a velocity resolution of 1.3 km s^{-1}, and local emission unrelated to the Carina arm is shown dotted.

lanes as seen on optical pictures (see, e.g., the image in The Messenger 67, 1992, P14). It can be followed continuously over more than 8 kpc, and is best defined in the upper part of the map where its width (at half maximum, corrected for inclination) is about 0.5–1.5 kpc. Owing to its larger arm-interarm contrast, the CO emission appears to be a significantly sharper tracer of spiral structure than the H I (Fig. 2). Although the ratio of the strongest CO peak to the regions well outside the molecular arm can be higher than 20:1, the mean CO arm-interarm contrast found by averaging the spectra within the nine bins used to produce Figure 2 (see caption) is about 10:1. The H2 contrast could of course be lower if small clouds systematically colder than those in the arms were present in the interarm region (Cohen et al. 1980).

The strongest peaks of CO emission are associated in both space (Fig. 1) and velocity (Fig. 3) with strong peaks of H I. The molecular and atomic gas appear to share the same kinematics (Fig. 3), although the H I shows a second velocity component at higher velocity, attributed to the warped outer disk of the galaxy seen in projection on the inner disk (Brinks & Burton 1984); this component is not seen in CO, at least at the sensitivity of the present survey. The velocity structure of the arm at $Y \leq 4'$ is similar, with no systematic offset apparent between the CO and the H I.

At our linear resolution, the structure of the upper part of the molecular arm S4 in M31 is remarkably similar to that portion of the Carina spiral arm in our Galaxy lying at the same galactic radius (Fig. 4). Large complexes of molecular gas with sizes of a few hundred parsecs and masses (deduced from the CO luminosity) in excess to $10^6\ M_\odot$ are seen in both maps, and CO profiles averaged over these complexes have roughly the same peak temperatures and linewidths (Fig. 4 inserts). The full-resolution maps of the Carina arm (Grabelsky et al. 1988) show that these large complexes typically correspond to a few blended GMC's; the situation is quite probably the same in M31. The striking similarity between S4 and the Carina arm suggests that the physical conditions of the molecular gas are probably quite similar in the two cases, and that the conversion factor X between CO emission and H_2 column density, in particular, is unlikely to be very different in this region of M31 than in the Carina arm of the Milky Way. It should be pointed out however, that while S4 is one of the brightest CO spiral arms in M31, the Carina arm in the Milky Way is relatively dim compared with the arms at smaller Galactic radii, i.e., in the molecular ring at R ~ 4–6 kpc.

The bright OB associations OB 6, 4, 7, 13, and 14, most conspicuous in the far-UV map (Fig. 1*d*), are evidently part of the large spiral arm we observe in CO, but they are systematically displaced from both the gas and dust by about 500 pc. Several fainter associations (OB 2, 1, 3, 5 and 10) are seen even further from the arm. They are not conspicuous in the far-UV map, contain only a few scattered H II regions and are therefore likely to be older associations. Three small associations (OB 15, 16, and 18) are associated with S3 at $X \sim -32'$, $Y \sim +4'$; they are aligned with the gaseous feature. It is worth noting that OB 13 (NGC 206) and less clearly OB 4, 6, and 7 have apparently evacuated the local interstellar medium, both atomic and molecular (Figs. 1*a*, 1*b*; see Brinks & Bajaja 1986); probably the result of stellar winds and supernovae explosions associated with the OB associations. The lower part of the arm S4 studied here is less well defined and contains many more OB associations than the upper part. It is likely that the more perturbed structure observed in the lower part is also the result of the stellar winds or supernovae explosions (or both) associated with the vigorous star-forming activity observed there.

Most of the H II regions, except for the few directly linked to OB 13 and OB 9, are found along the edge of the main gaseous arm that faces the OB associations (see for instance the strings of H II regions at $X \sim -47'$, $Y \sim +5'$ and $X \sim -43'$, $Y \sim +9'$). Altogether, they define an arm intermediate between the gaseous arm and that traced by the OB associations.

The offset between the gaseous spiral arm and that defined by the H II regions is about 200 pc (see Fig. 2). The H II regions found around $X \sim -32'$, $Y \sim +4'$ delineate the segment of spiral arm S3; there, no displacement between the gaseous spiral arm and the distribution of the H II region is apparent. Similar offsets between the gas and Population I objects (H II regions and OB associations) have been observed in a few other nearby galaxies (e.g., M33, Courtés & Dubout-Crillon 1971 or M51, Vogel, Kulkarni, & Scoville 1988), and have been interpreted as resulting from the propagation of a spiral density wave which had triggered star-formation: the OB associations may have dispersed the gas left over after star-formation, while the shock moved further on, compressing the gas in the observed gaseous spiral arm.

Although the value of the mass calibration ratio $X = N(H_2)/W_{CO}$ between the CO integrated intensity and the H_2 column density is so far poorly determined in M31, a value close to the Galactic one is suggested both by interferometric observations of individual giant molecular clouds in the ring of M31 (e.g., Vogel, Boulanger, & Ball 1987) and by the present work (Fig. 4). In the absence of a better estimate, we will use the value of $X = 1.9 \times 10^{20}$ cm^{-2} (K km s^{-1})$^{-1}$ determined for the Milky Way by Strong et al. (1988, corrected to the T_{mb} scale). The CO(1–0) integrated intensity averaged over the entire map (Fig. 1*a*) is 1.25 K km s^{-1}. This yields an average H_2 surface density of 0.80 $M_\odot$ pc^{-2} (corrected for inclination), and a total molecular mass of 6×10^7 $M_\odot$ in the region studied. Under the assumption that the H I line at 21 cm is optically thin, the mass surface density of H I is readily calculated from the integrated intensity of the 21 cm line. From the Westerbork H I data, we have determined a 21 cm line integrated intensity averaged over the same region of 235 K km s^{-1}, which yields an average mass surface density of 0.75 $M_\odot$ pc^{-2} (corrected for inclination) and a total mass of atomic gas comparable to that of H_2. Inside the large condensations defined on Figure 4, the average mass surface density of H_2 increases to about 3 $M_\odot$ pc^{-2}, and that of H I to 2 $M_\odot$ pc^{-2}.

4. CONCLUSION

Two molecular arms, one remarkably long and well defined, coincident with atomic gas and dust features, are clearly revealed by our present CO observations of the southern tangent of the Population I ring in M31. The main gaseous arm (S4) is offset by about 500 pc from the arm traced by the OB stars, possibly as the result of displacement by a large-scale shock which has triggered the formation of the OB associations. Most of the H II regions lie along the interface between the OB associations and the gaseous arm. The main molecular concentrations along S4 are remarkably similar in size and CO intensity to those in the Carina arm of the Milky Way at the same Galactic radius. The Galactic molecular arms at smaller radii are however much brighter in CO than the Carina arm, whereas S4 is one of the brightest arm in M31.

We are grateful to Dr. E. Brinks who provided the H I data cube, to Dr. B. Milliard who provided the UV image of M31 and to Dr. G. Helou who kindly made the high-resolution *IRAS* maps of M31 available to us. We thank Dr. S. Xie and Dr. M. Heyer for their help with the observations, and the FCRAO program committee for their award of observing time. L. L. and E. K. thank the CfA for travel support.

REFERENCES

Baade, W. 1958, Specola Astron. Vaticana Ric. Astron., 5, 3
Brinks, E., & Bajaja, E. 1986, A&A, 169, 14
Brinks, E., & Shane, W. W. 1984, A&AS, 55, 179
Cohen, R. S., Cong, H., Dame, T. M., & Thaddeus, P. 1980, ApJ, 239, L53
Courtés, G., & Dubout-Crillon, R. 1971, A&A, 11, 468
Dame, T. M., Koper, E., Israel, F. P., & Thaddeus, P. 1993, ApJ, 418, 730
Grabelsky, D. A., Cohen, R. S., Bronfman, L., & Thaddeus, P. 1988, ApJ, 331, 181
Kutner, M. L., Verter, F., & Rickard, L. J. 1990, ApJ, 365, 195
Magnier, E. A., Battinelli, P., Lewin, W. G. H., Haizman, Z., van Paradijs, J., Hasinger, G., Pietsch, W., Supper, R., & Trumper, J. 1993, A&A, 278, 36
Milliard, B. 1984 Ph.D. thesis, Univ. Marseille
Pellet, A., Astier, N., Courtes, G., Maucherat, A., Monnet, G., & Simien, F. 1978, A&AS, 31, 439
Stark, A. A., Linke, R. A., & Frerking, M. A. 1981, BAAS, 13, 535
Strong, A. W., Bloemen, J. G. B. M., Dame, T. M., Grenier, I. A., Hermsen, W., Lebrun, F., Nyman, L. A., Pollock, A. M. T., & Thaddeus, P. 1988, A&A, 207, 1
Vogel, S. N., Boulanger, F., & Ball, R. 1987, ApJ, 321, L145
Vogel, S. N., Kulkarni, S. R., & Scoville, N. 1988, Nature, 334, 402
Xu, C., & Helou, G. 1995, *IRAS* prepr. No. 127